

⁴T. H. Geballe and F. J. Morin, Phys. Rev. **95**, 1085 (1954).

⁵S. H. Koenig, J. Phys. Chem. Solids **8**, 227 (1959).

⁶P. J. Price (unpublished).

⁷P. Fisher and H. Y. Fan, Bull. Am. Phys. Soc. **3**, 128 (1958).

⁸S. H. Koenig, Phys. Rev. **110**, 988 (1958).

⁹See W. S. Boyle and K. F. Rodgers, Jr., J. Opt. Soc. Am. **49**, 66 (1959).

¹⁰M. A. Lampert, Signal Corps Report (unpublished).

¹¹E. Burstein, J. S. Picus, and N. Sclar, Proceedings of the Conference on Photoconductivity, Atlantic City, November 4-6, 1954, edited by R. G. Breckenridge et al. (John Wiley and Sons, Inc., New York, 1956), p. 353.

¹²S. H. Koenig, Phys. Rev. **110**, 986 (1958).

¹³A. Karagounis, Suppl. Bull. inst. intern. froid, Annexe 1956-2, p. 195.

INTERNAL IMPURITY LEVELS IN SEMICONDUCTORS: EXPERIMENTS IN *p*-TYPE SILICON*

Solomon Zwerdling, Kenneth J. Button, Benjamin Lax, and Laura M. Roth
Lincoln Laboratory, Massachusetts Institute of Technology, Lexington, Massachusetts
(Received December 29, 1959)

The concept of the existence of multiple sets of localized impurity levels, each associated with the various band extrema pertinent to its donor or acceptor character, has been verified by the observation of newly-found transitions to acceptor excited states in silicon lying near the split-off $p_{1/2}$ valence band maximum, within the continuum of the $p_{3/2}$ bands as shown in Fig. 1. The detection of such discrete internal impurity levels should provide information about the location of higher bands in energy-momentum space as well as about their characteristics and band parameters.

In the case of the impurity levels of the valence bands in silicon, transitions are possible between the ground state, which is primarily associated with the $p_{3/2}$ band (band *a*), and the excited states of the $p_{1/2}$ band (band *b*), as shown in Fig. 1. If we treat the coupling between the $p_{3/2}$ and $p_{1/2}$ bands as a perturbation, the transition probability from level 1 of band *a* to level 2 of band *b* has the form

$$W \propto \left[\vec{\Pi}'_{a(1)b(2)} + \frac{\mathcal{H}'_{a(1)b(1)}}{\mathcal{E}_{a(1)b(1)}} \vec{\Pi}_{b(1)b(2)} - \frac{\mathcal{H}'_{a(2)b(2)}}{\mathcal{E}_{a(2)b(2)}} \vec{\Pi}_{a(1)a(2)} \right]^2 \quad (1)$$

Here $\vec{\Pi}$ is a momentum operator between ground and excited states,¹ \mathcal{H}'_{ab} is a matrix element of the effective-mass Hamiltonian connecting the two bands, and \mathcal{E}_{ab} is the energy separation of the levels. Transitions are also allowed between the ground state of band *b* to an excited state of band *a* permitting, in principle, population inversion between state 2 and state 1 of band *b* or

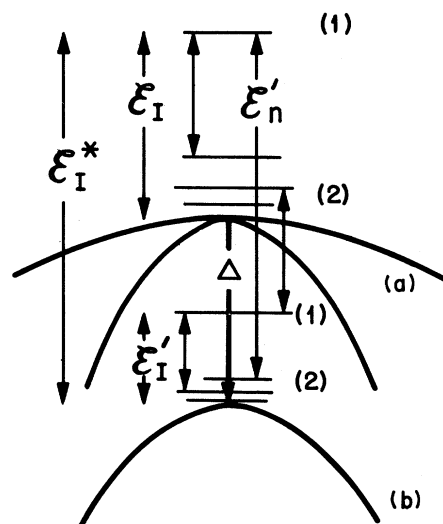


FIG. 1. Valence energy bands of silicon showing the acceptor ground state (1) and excited states (2) for both the degenerate $p_{3/2}$ bands (*a*) and the split-off $p_{1/2}$ band (*b*). The "internal" impurity levels are those nearest band *b*. The unlabeled arrows are also allowed transitions.

between state 1 of band *b* and state 2 of band *a*.

Optically-induced transitions of holes from the ground state in the forbidden gap to excited states associated with the split-off $p_{1/2}$ valence band were observed at 4°K in the wavelength range 10-15 microns using both boron- and aluminum-doped silicon. The spectra for boron-doped silicon in Fig. 2 show clearly-defined absorption maxima for transitions to the first few quantum levels, and the energies appeared to fit a Rydberg series for both boron and alumi-

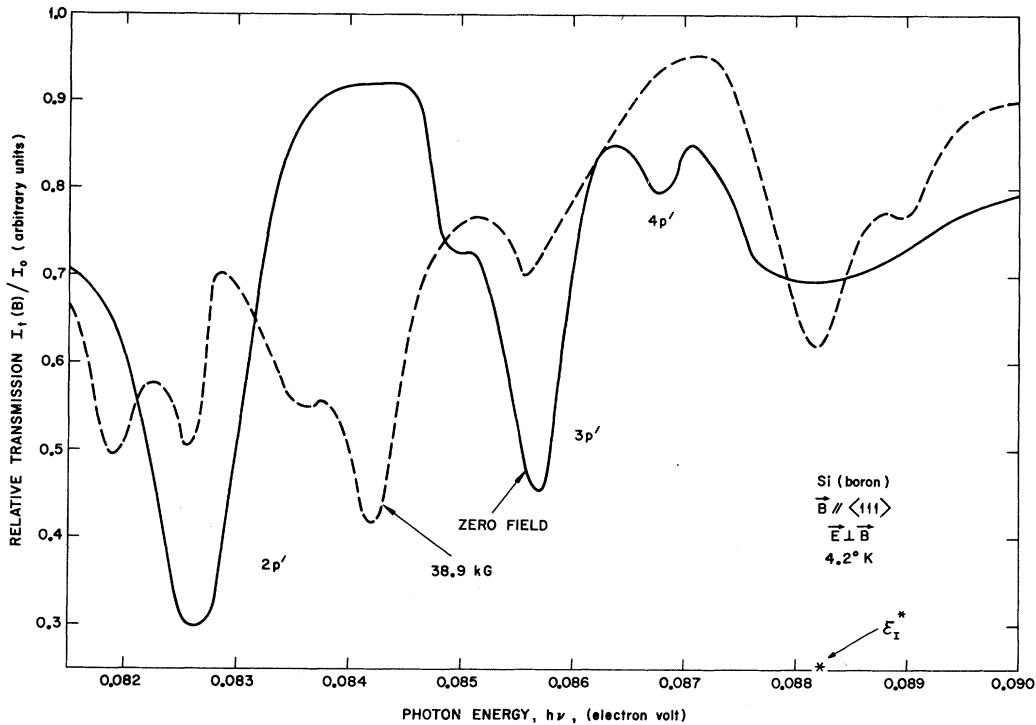


FIG. 2. Experimental spectrum obtained for the transitions at zero field (solid line) and at 38.9 kilogauss (dashed line) from the boron acceptor ground state in the gap to the internal excited states of the $p_{1/2}$ band. The ordinate scale is the ratio of the transmission through a doped sample ($t = 3$ mm, $N_A = 6 \times 10^{15}$ /cc) to that of a pure sample.

num impurities in accordance with $\varepsilon_n' = \varepsilon_I^* - \varepsilon_I'(1/n^2)$, where $\varepsilon_I' = (ry/\kappa^2)(m^*/m_0)$. However, it is necessary to include a correction for the nonparabolic character of the $p_{1/2}$ valence band, so that the relationship becomes

$$\varepsilon_n' = \varepsilon_I^* - \varepsilon_I' \left[\frac{1}{n^2} - \lambda \left(\frac{8}{3n^3} - \frac{3}{n^4} \right) \right], \quad (2)$$

where $\lambda = [2(B^2 + \frac{1}{5}C^2)/A^2][\varepsilon_I'/\Delta] = 0.339$. The effective-mass Hamiltonian for the $p_{1/2}$ band was expanded to include the p^4 momentum term,² and then a perturbation theory calculation of the expectation value of the latter was taken using np' wave functions. The coefficient λ is essentially the dimensionless coefficient of the p^4 term. A , B , and C are the valence band parameters³ and Δ is the spin-orbit splitting of the valence bands. In the plot of Eq. (2) shown in Fig. 3, the ordinate scale for the aluminum acceptor is shifted relative to that of the boron acceptor by just the greater depth of its gap ground state. The intercept on the energy ordinate gives directly ε_I^* (boron) = (0.0882 ± 0.0001) eV and ε_I^* (aluminum) = (0.1130 ± 0.0001) eV.

From previous infrared spectral measurements⁴ on acceptor excited states in silicon, the ionization energy of holes to the $p_{3/2}$ band maximum can be estimated by extrapolating the transition photon energies to a "limit," giving ε_I^* (boron) = (0.0441 ± 0.0003) eV and ε_I^* (aluminum) = (0.0690 ± 0.0002) eV. Then the spin-orbit splitting of the valence bands in silicon⁵ is

$$\Delta = \varepsilon_I^* - \varepsilon_I = (0.0441 \pm 0.0004) \text{ eV}. \quad (3)$$

In evaluating λ for plotting Fig. 3, we have used $m^* = 0.25m_0$ deduced from microwave cyclotron resonance results,³ and the value of Δ obtained from a plot of the uncorrected Rydberg formula (dashed line shown in Fig. 3) in the manner described above. This determination of Δ gave the same value as in Eq. (3), and is valid since the entire Rydberg correction term vanishes as $1/n^3$ as $n \rightarrow \infty$, so that both the corrected and uncorrected plots yield the same series limit ε_I^* . From the expression for ε_I' , the hole effective mass for the $p_{1/2}$ valence band is found to be $m^* = (0.25 \pm 0.01)m_0$, where $ry = 13.6$ eV and a low-temperature value⁶ of $\kappa^2 = 130$ have

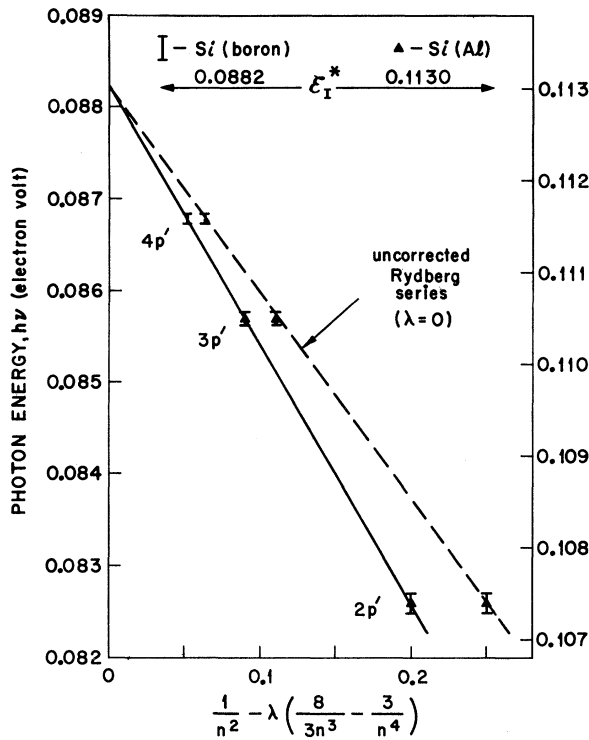


FIG. 3. Plot of Rydberg series (dashed line) and Eq. (2) (solid line) using experimental energy values for optical transitions from acceptor ground state in the forbidden gap to internal acceptor excited states for boron-doped Si (left scale) and Al-doped Si (right scale). For Si(boron), $N_A = 6 \times 10^{15}/\text{cm}^3$ and $t = 3$ mm, and for Si(Al), $N_A = 2 \times 10^{15}/\text{cm}^3$ and $t = 6$ mm.

been used. This mass value is in good agreement with the cyclotron resonance result.³ If the p^4 term were not included, this hole effective mass would be $0.205m_0$, indicating a correction of about 20% due to the influence of the $p_{3/2}$ bands.

The Zeeman effect of these internal excited states is shown in Fig. 4 and, in addition, transitions apparently associated with bound Landau levels within the $p_{1/2}$ band are evident above \mathcal{E}_I^* . The spectral structure associated with the transition to the $2p'$ level is probably due to spin splitting superimposed on the Zeeman splitting. Similar spin splitting may be present in the bound Landau level spectra. Since the gap ground state presumably has a Zeeman effect also, further investigation will be needed for confirmation as well as for an evaluation of the $p_{1/2}$ band effective mass from the magnetospectroscopic data. Tentatively, the interpretation as spin splitting yields $g \approx 3$. It may also be possible to determine the sign of the valence band parameter B from this g value.

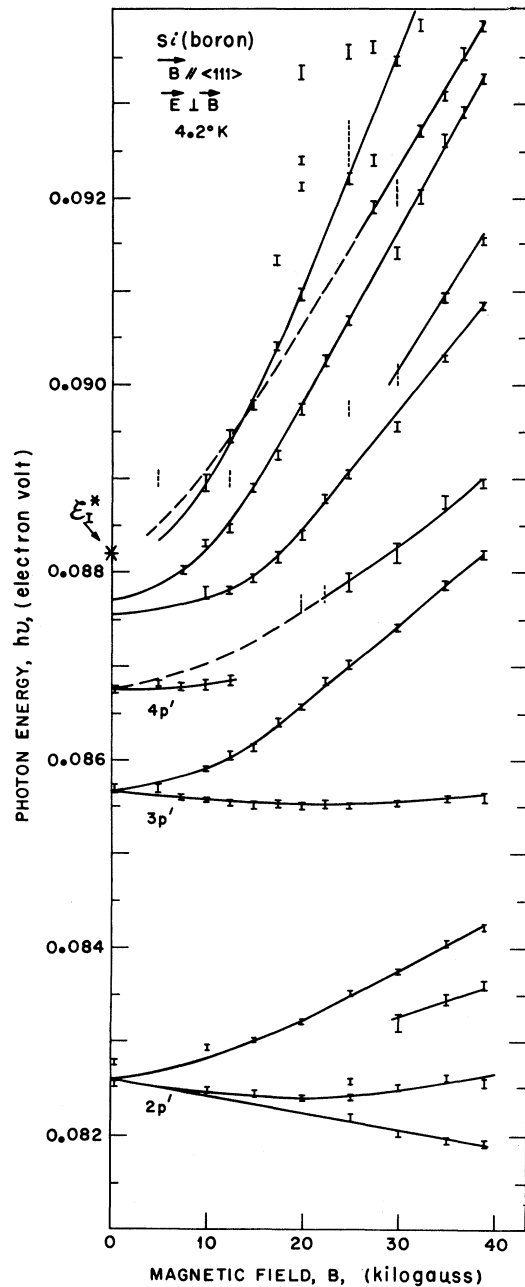


FIG. 4. Zeeman-effect energy level diagram showing the splitting of the internal impurity levels in a magnetic field. With increasing magnetic field the highest states become linearly dependent on field above the ionization limit, similar to Landau levels. The transition to the $2p'$ level shows structure probably due to spin splitting.

An analogous experiment should be possible for the valence bands in p -type germanium. Here the values of \mathcal{E}_{ab} would be larger by a factor of about four, and the first term of Eq. (1)

is dominant. The transition probability should be of the same order of magnitude as in Si. Unfortunately, the absorption corresponding to this transition overlaps by ~ 0.01 eV the steep absorption edge of the intervalence band transition at ~ 0.28 eV. Nevertheless, by using an optimum impurity concentration and high spectral resolution, it may be possible to observe this transition in Ge as well as in InAs, GaAs, InP, GaP, AlP, AlAs, and AlSb where intervalence band transitions have been studied.⁷

In principle, it should be possible to observe transitions between impurity levels of bands having extrema at different values of \vec{k} . Such an indirect process probably involves the emission of phonons at low temperature. Thus in heavily-doped *n*-type Ge, transitions from the lowest $\langle 111 \rangle$ impurity level to the $\langle 000 \rangle$ and $\langle 100 \rangle$ impurity states may be observable. The former should occur at ~ 0.15 eV,⁸ and the latter at ~ 0.22 eV.⁹ Similarly in GaSb, a transition from the $\langle 000 \rangle$ to the $\langle 111 \rangle$ impurity level should occur at ~ 0.08 eV.¹⁰ However, since the transition probability is low, impurity concentrations of the order of $10^{19}/\text{cm}^3$ may be required.

We have profited greatly from theoretical dis-

cussions with Professor G. F. Koster.

*This work was performed with the joint support of the U. S. Army, Navy, and Air Force.

¹G. F. Koster has shown that the operator $\bar{\Pi}$ is given by $\bar{\Pi} = m_0 \nabla_p \mathcal{H}$, where \mathcal{H} is either the 4×4 or the 2×2 effective-mass Hamiltonian corresponding to $\bar{\Pi}_a$ or $\bar{\Pi}_b$. The operator $\bar{\Pi}'$ is similarly obtained from \mathcal{H}' , which is associated with the overlapping elements of the 6×6 matrix.

²E. O. Kane, *J. Phys. Chem. Solids* **1**, 82 (1956).

³R. N. Dexter, H. J. Zeiger, and B. Lax, *Phys. Rev.* **104**, 637 (1956).

⁴H. J. Hrostowski and R. H. Kaiser, *J. Phys. Chem. Solids* **4**, 148 (1958); S. Zwerdling, K. J. Button, and B. Lax (to be published).

⁵A rough estimate of $\Delta \sim 0.05$ eV has been made from measurements of intervalence band transitions by L. Huld and T. Staflin, *Phys. Rev. Letters* **1**, 313 (1958).

⁶Based on the data of M. Cardona, W. Paul, and H. Brooks, *J. Phys. Chem. Solids* **8**, 204 (1959).

⁷R. Braunstein, *J. Phys. Chem. Solids* **8**, 280 (1959).

⁸S. Zwerdling, B. Lax, L. M. Roth, and K. J. Button, *Phys. Rev.* **114**, 80 (1959).

⁹R. Braunstein, A. R. Moore, and F. Herman, *Phys. Rev.* **109**, 695 (1958).

¹⁰A. Sagar, Westinghouse Research Report 6-40602-3P5, June, 1959 (unpublished).

UPPER LIMIT FOR THE ANISOTROPY OF INERTIA FROM THE MÖSSBAUER EFFECT*

G. Cocconi[†] and E. E. Salpeter
Cornell University, Ithaca, New York
(Received January 21, 1960)

The question of anisotropy of inertia has been discussed in some detail in a previous paper¹; here we recall only that one of the consequences of Mach's principle could be that the value of the inertial mass M of a body depends on whether its acceleration is in the direction towards the center of our galaxy or in a direction perpendicular to it. The variation ΔM of mass with direction, if it exists, was found to satisfy $\Delta M/M < 10^{-9}$.

The recent discovery of the Mössbauer effect² has opened the possibility of comparing frequencies of γ rays, emitted by long-lived states of nuclei, with extremely high precision. The recoil-free resonant absorption of the 14-keV nuclear γ ray of Fe⁵⁷ has already been investigated^{3,4} with sufficient resolution to observe the hyperfine structure splitting in the excited state. The Mössbauer effect has been proposed as an

excellent tool for detecting the gravitational red shift⁵ and for many other purposes. Here we propose its use in a search for anisotropy of inertia. Precision studies of the line shapes of the Fe⁵⁷ transition, for instance, will serve this purpose if the atomic spins can be aligned, both in the emitter and in the absorber, and the orientation of the spins relative to the direction towards the Galactic center is varied.

Consider an Fe⁵⁷ nucleus in a nuclear state with total angular momentum quantum number J in a ferromagnetic sample with atomic spins aligned parallel to an external magnetic field. The effect of some anisotropy of inertia is then very similar to that discussed in reference 1 for the atomic Zeeman effect, except that we are now dealing with the motion of the nucleon in the Fe⁵⁷ responsible for the γ -ray transition (at least on a shell-model picture) instead of the